SAND TRANSPORT BY WAVES

By Jan van de Graaff* and
Wiel M.K. Tilmans

!. Introduction

In coastal engineering practice frequently a distinction is made between two different modes of sand transport:

- longshore transport
- onshore-offshore transport

From a theoretical point of view the longshore transport phenomenon is not as complicated as the onshore-offshore phenomenon. In the longshore mode of transport, the variations in time (wave period scale) are less important since the current velocity component in the longshore direction is nearly constant in time. In the onshoreoffshore direction both the time-variations of (orbital) velocities and sediment concentrations have to be considered in order to be able to compute the resulting net sediment transport. Since our quantitative knowledge of the time variations of the concentration is extremely poor at this moment, realistic calculations of the onshore-offshore transport, based on the actual physics involved, cannot be made. In many practical coastal engineering applications the onshore-offshore transports play an important role, however, and therefore a reliable description is urgently needed. Swart (1974;1976) presented an experimentally based computing method. The Coastal Engineering Group of the Delft University of Technology has been studying the onshoreoffshore transport phenomenon since 1968. Since the beginning of the investigation a rather experimental research method has been used also since the measuring devices lacked to measure real concentrations. The outcome of the present investigation, however, is rather surprising in some aspects. Bijker, Van Hijum and Vellinga (1976) reported on some preliminary results. Later series of tests resulted in a change of the

Senior Scientific Officer, Delft University of Technology;
 Civil Engineering Department; Coastal Engineering Group

^{**} Teaching Assistant Coastal Engineering Group
At present Project Engineer, Delft Hydraulics Laboratory;
De Voorst Laboratory.

preliminary ideas.

During the present investigation the (net) sediment transport due to waves over a horizontal sand bottom has been studied. Various grain sizes have been used for bottom material.

This paper describes some newer insights. The results at present can hardly be used for direct practical use. However, for a better understanding of the complex character of the onshore-offshore sediment transport, the test results are undoubtedly of interest.

This paper is a summary and uses the test results of the graduation theses of Vellinga (1975), Schepers (1978) and Tilmans (1979).

2. Small-scale tests

During the present experimental study, a wave-flume has been used in which regular waves can be generated (see Fig. 1). Over approximately 9 m the horizontal bed consists of well-sorted sand (see Fig. 2). At the "landward"-side of the flume a wave-absorbing slope has been constructed. The 1:10 slope is rather steep, resulting in some wave reflection.

In TABLE I a summary of the boundary conditions has been given. (In the present paper only tests with T = 1.7 s have been considered).

D ₅₀	h	H/h	source
(µm)	(m)	. (-)	
87	.20; .25; .30	.20; .25	Tilmans (1979)
185	[.30; .35	
125	.30	.30	Schepers (1978)
465			
250	.20; .25; .30	.20; .30	Vellinga (1975)
		.40	

All tests T = 1.7 s.

TABLE I Boundary conditions

- S (10-6m3/ms)

.26 .24 .24 (\$/\varepsilon\).22 1.18 20

80. % 80. %

° 04

.026

40 r

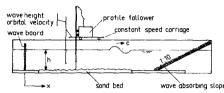


Fig.1 Sketch of wave flume.

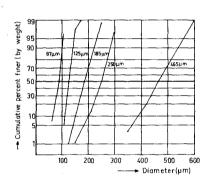
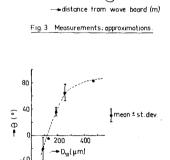


Fig.2 Grain size distribution.



T 185-- 8

(ů,

 $\left[\overline{\gamma}\right]$

Fig 5 Effect of D_{50} on Θ

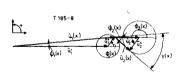


Fig. 4 Vector summation first and second harmonics

Sediment transport

Before and after a test the bottom profile was measured with an electronic "bottom profile follower". The profile follower was attached to a constant speed carriage. It could be arranged by some electronics that the total volume of sand within 0.25 m sections was measured. By integrating the total volume of sand from the sand-less part of the bottom in front of the wave-penerator to the sand-less part in front of the wave-absorbing slope and subtracting these values after and before a test, the net sediment transport at 0.25 m intervals could be computed (Fig. 3 gives an example). The bed profile was measured in three lines along the length of the flume; the mean value has been taken into account. Sometimes a slight adjustment was necessary to correct the differences in amount of material before and after a test. Normally the tests had a duration of 30 minutes.

Wave-heights

The form of the surface-elevation has been measured at cross-sections at 0.25~m intervals. A resistance type wave gauge was used for this purpose.

Water-motion

At 1/3 of the water depth (h) above the bottom the horizontal component of the orbital velocity was measured at the cross-sections at 0.25 m intervals with a micro-propeller. The propeller signal was sampled with a constant time-step. About 8 samples were obtained within a wave period.

The several harmonic components were determined afterwards with a harmonic analysis computer program:

$$u(t) = u_0 + \hat{u}_1 \cos \omega t + \hat{u}_2 \cos(2\omega t + \gamma) + \dots$$
 (1)

where: u(t): the momentary horizontal component of the orbital velocity; \mathbf{u}_0 : mean resulting velocity; $\hat{\mathbf{u}}_1$, $\hat{\mathbf{u}}_2$: first and second harmonic components; ω : wave frequency; t: time and γ : phase

angle between the first and second harmonic component.

As can be seen from Fig. 3 the magnitude of the components $\hat{\mathbf{u}}_1$ and $\hat{\mathbf{u}}_2$ of Eq. 1 varies along the axis of the flume. That indicates the occurrence of secondary waves. Hulsbergen (1974) and Buhr Hansen and Svendsen (1974) described some aspects of the secondary wave phenomenon. The selected boundary conditions for the present study (especially the h/λ -values) are as such, that secondary waves do occur.

3. Test results

3.1. Theoretical considerations

Wave types

Due to the selected boundary conditions (see TABLE I) and the manner of wave generation (wave-paddle sinusoidally moving) various "waves" and hence orbital velocity components can be distinguished in the flume, viz.:

- main wave (third order Stokes wave)
- secondary wave (Fontanet wave)
- interaction waves

[See Kravtchenko and Santon (1957); Fontanet (1961); Hulsbergen (1974)]

The horizontal component of the orbital velocity under a third order Stokes wave can be described as:

$$\mathbf{u}(\mathsf{t}) = \hat{\mathbf{u}}_1^{\mathsf{t}} \cos \omega \mathsf{t} + \hat{\mathbf{u}}_2^{\mathsf{t}} \cos 2\omega \mathsf{t} + \hat{\mathbf{u}}_3^{\mathsf{t}} \cos 3\omega \mathsf{t} \tag{2}$$

where: $\widehat{u}_1^{\, \text{t}}, \ \widehat{u}_2^{\, \text{t}}$ and $\widehat{u}_3^{\, \text{t}};$ the Stokes components.

Due to the disagreements in velocity profile of a gravity wave and the translating wave board a "free" secondary wave (Fontanet wave) is generated. This wave with a frequency 2ω moves, contrary to the second order Stokes component with the same frequency, "free" with its own wave propagation speed through the wave flume. The corresponding maximum horizontal orbital velocity component is indicated by \hat{u}_{2}^{\star} .

Due to non-linear interaction of the Stokes and the Fontanet waves, so-called interaction waves are generated. For the present analysis the interaction waves with the frequencies ω and 3ω are important. Both interaction waves have propagation speeds which are different from the "normal" celerities with respect to the frequencies. The orbital components are indicated by \widehat{u}_{3}^{\star} and \widehat{u}_{3}^{\star} .

As a result of the foregoing consideration each of the three basic Stokes components has thus a counterpart with the same frequency but with a different celerity. The various components are summarized in TABLE II.

Frequency	Stokes components		Interaction/Fontanet components				
	orbital velocity	celerity	orbital velocity	celerity			
ω 2ω 3ω	û' 1 û' 2 û' 3	c ₁ c ₁	û* û* û* û* 2*	c * c 2 c ' *			

TABLE II Wave components

When two waves are present in a wave flume with the same frequency but with a different celerity, the phase difference ϕ between such two waves at a certain position x can be found again at the position $x + L_{OV}$ in which L_{OV} is the so-called overtake length defined as:

$$L_{ov} = \frac{\text{wave length slow wave}}{\text{celerity difference}} \cdot \text{celerity fast wave}$$

Thus for the second harmonic components results:

$$L_{ov2} = \frac{\lambda_2}{c_1 - c_2} \cdot c_1$$
 (3)

With $c_1 = \lambda_1/T$ and $c_2 = 2\lambda_2/T$, Eq. (3) yields:

$$L_{ov2} = \frac{\lambda_1 \lambda_2}{\lambda_1 - 2\lambda_2} \tag{4}$$

It can be proven that, with the theoretical values of $c_{\frac{1}{x}}$ and $c_{\frac{1}{x}}^{1}$ (see TABLE II) for both L_{ov1} and L_{ov3} the same length as L_{ov2} results (= L_{ov}).

At the position x where ϕ_i = 0° both components yield a resulting \hat{u}_i component with magnitude:

$$\hat{\mathbf{u}}_{i} = \hat{\mathbf{u}}_{i}^{\dagger} + \hat{\mathbf{u}}_{i}^{\star} \tag{5}$$

(i = 1, 2, 3).

Where $\phi_i = 180^{\circ}$, results:

$$\hat{\mathbf{u}}_{i} = \hat{\mathbf{u}}_{i}^{!} - \hat{\mathbf{u}}_{i}^{*} \tag{6}$$

From the measurements of Fig. 3 it can be seen that for the first and the second harmonic component seemingly the same $L_{\rm ov}$ is found. Furthermore, it can be detected that where $\phi_1=0^\circ$, $\phi_2\approx180^\circ$ results and vice versa. Fontanet (1961) did prove this theoretically. In Fig. 4 the resulting vector summation of the first and the second harmonic component is given. From that figure the expression for $\hat{u}_1(x)$ (i =1, 2) becomes:

$$\hat{\mathbf{u}}_{i}(\mathbf{x}) = \sqrt{(\hat{\mathbf{u}}_{i}^{t})^{2} + (\hat{\mathbf{u}}_{i}^{*})^{2} + 2\hat{\mathbf{u}}_{i}^{t} \hat{\mathbf{u}}_{i}^{*} \cos \phi_{i}(\mathbf{x})}$$
(7)

where:
$$\phi_1(x) = \frac{x - x_1 top}{L_{ov}} * 360^{\circ}$$
 (8)

$$\phi_2(x) = \frac{x - x_{1 \text{top}}}{L_{ov}} * 360^{\circ} + 180^{\circ}$$
 (9)

 $x_{1top} = x$ -ordinate where top in \hat{u}_1 -curve occurs.

Since the u_0^- , \hat{u}_3^- and further components in Eq. (1) turned out to be insignificantly small, they will be ignored in further analyses; thus only the first and the second harmonic components remain.

Sediment transports

Till now no sound physical description of the sediment transport as a

function of the water motion is known. It can be seen from Fig. 3 that the net sediment transports as a function of x do vary apparently with the same overtake length, $L_{\rm ov}$, as the orbital components vary.

3.2. Results

As can be seen from Fig. 3 the actual test results show the general trends as discussed in section 3.1 quite well. Some fluctuations do occur however. For instance fluctuations due to measuring errors or wave reflection. In the further analyses it is usefull to use mathematical descriptions for the water motion-($\hat{\mathbf{u}}_1$, $\hat{\mathbf{u}}_2$) and transport-(S) parameters as a function of x. The basic measurements of the Various tests (compare the measuring points of Fig. 3) have been approximated by three different curves with a least squares fitting-method. For the $\hat{\mathbf{u}}_1$ - and $\hat{\mathbf{u}}_2$ -curves an equation according to Eq. (7) was used. For the overtake length the theoretical values which can be computed with the help of the third order wave theory of Skielbreia (1958), have been taken into account. In Eq. (7) three parameters, \hat{u}_i^t , \hat{u}_i^{\star} and the position of $x_{|top}$ are to be approximated. TABLE III gives the results of the various tests. In Fig. 3 the ultimate approximationcurves have been given also. From TABLE III it can be seen that the maximum of the $\hat{\mathbf{u}}_1$ -curve and the minimum of the $\hat{\mathbf{u}}_2$ -curve (= max $\hat{\mathbf{u}}_2$ -curve $\frac{+}{2}$ L_{OV}) are indeed nearly on the same x-position. In the further analyses the mean of the x_{ltop} and $x_{2trough}$ position is taken into account (XTU in TABLE III).

The sediment transport curve, S(x), has been approximated by a simple cosine-function with the overtake length L_{ov} as basis:

$$S(x) = \overline{S} + \hat{S} \cos \left(\frac{x - x_{1 \text{top}}}{L_{\text{ov}}} * 360^{\circ} - \theta \right)$$
 (10)

where: \overline{S} : mean sediment transport; \hat{S} : amplitude of the transport variation and θ : phase shift of the S(x)-curve top with respect to the position of $x_{1\text{top}}$. Positive transport is in wave propagation direction.

For the time being the cosine-function has been adopted for simplicity reasons; no physical argument is known as yet. The \overline{S} -, \hat{S} - and θ -values

Test	û'i	û *	ũ;	û ₂ *	s	ŝ	* _{1tp}	x _{2tr}	XTU	XTS	Lov	θ
		(m/	s)		(10 ⁻⁶	m ³ /ms)		(m)				(°)
T 87-1 T 87-2 T 87-3 T 87-4 T 87-5 T 87-6 T 87-7 T 87-8 T 87-9 T 87-10 T 87-11	.135 .147 .138 .182 .185 .183 .194 .191 .227 - .233 .238	.011 .006 .002 .026 .014 .012 .037 .025 .024 -	.029 .026 .018 .058 .040 .031 .070 .046 .041 -	.015 .013 .011 .025 .022 .036 .036 .034 -	18 10 03 80 21 .26 87 .09 .30	.23 .32 .08 1.87 1.44 1.25 3.39 3.17 2.61 - 6.31 5.37	5.53 4.84 8.99 4.80 9.47 8.42 10.17 9.02 7.57 - 8.91 8.14	5.35 4.49 8.98 4.55 9.36 8.35 10.06 9.07 7.42 - 8.80 8.11	5.44 4.67 8.99 4.68 9.42 8.39 10.12 9.05 7.50 - 8.86 8.13	3.98 8.42 4.47 9.03 8.28 9.86 8.97 7.38	4.67 5.68 5.08 4.54 5.43 4.88	-47 -44 -13
T125-1	.193	.028	.030	.028	37	1.13	8.42	8,53	8,47	8.42	4.41	- 4
T185-1 T185-2 T185-3 T185-4 T185-5 T185-6 T185-7 T185-9 T185-9 T185-10 T185-11	.149 .157 .146 .186 .193 .194 - .217 .208 - .235 .242	.010 .007 .004 .028 .016 .010 - .026 .016 - .040	.039 .032 .022 .055 .049 .033 - .058 .041	.016 .016 .015 .019 .026 .025 - .037 .028 - .049	.01 10 .01 74 66 31 84 29 -1.77	.71 - 2.55 2.01	5.31 4.67 9.01 4.59 9.26 8.48 - 8.80 8.39 8.80 8.28	5.34 4.46 9.06 4.80 9.31 8.54 - 8.88 8.42 - 8.84 8.39		8.78 -		30 46 32 51 34 37 - 34 30 - 33 31
T250-10 T250-11 T250-12 T250-13 T250-14 T250-15 T250-16 T250-17 T250-18 T250-19	.111 .163 .190 .137 .185 .232 .155 .203 .250 .190	.006 .018 .023 .006 .009 .014 .005 .014 .018 .021	.035 .060 .073 .037 .051 .071 .035 .052 .064 .026	.011 .025 .031 .012 .019 .018 .008 .012 .022 .026	.00 08 62 03 50 55 16 18 80 .01	.00 .39 1.60 .15 .53 1.90 .17 .62 1.62	5.53 5.63 5.58 4.74 5.07 4.60 4.27 4.16 4.49 8.60	6.00 5.64 5.79 5.36 5.26 5.17 4.43 4.23 4.51 8.67	5.77 5.64 5.69 5.05 5.17 4.89 4.35 4.20 4.50 8.64	- 6.41 6.38 6.42 5.94 5.77 5.09 4.98 5.29 9.49	5.98 5.43 4.93 5.27 4.88 4.52 4.67 4.41 4.41	51 50 94 57 70 57 64 69 69

TABLE III Summary of harmonic components of orbital velocity and transport components.

```
- transverse oscillations
```

T87-1: Test 1 with D_{50} = 87 μm

 $x_{ltp} = x_{ltop}$

 $x_{2tr} = x_{2trough}$

for the various tests have been included in TABLE III.

A visual inspection of figures like Fig. 3 learned that indeed the sediment transport in the flume can be described according to Eq. (10). In particular the \overline{S} -components did not show a trend as to be a function of the x-ordinate.

4. Mutual relationships

The objective of this study is to find relationships between the sediment transport and the water motion. In the further analyses the following hypotheses have been adopted:

- A direct relationship does exist between the sediment transport at a certain position x and the horizontal orbital velocities at the same x-ordinate.
 - E.g. the gradients in both S- and $\widehat{\mathbf{u}}$ -curves do not play a significant role.
- The water motion can be described sufficiently with only the first and second harmonic component.
- The velocities at 1/3 of the water depth above the bottom are considered to be crucial for the sediment transport.

In the next sections some examples of mutual relationships between sediment transport and water motion have been given.

4.1. Effect of D50 on θ

From TABLE III it can be seen that the phase shift θ of the top of the S-curve with respect to the top of the \hat{u}_1 -curve, varies apparently with the D_{50} -value. The θ -value is defined as:

$$\theta = \frac{XTS - XTU}{L_{ov}} * 360^{\circ}$$
 (11)

Although the variation in θ -values for a specific bed material is rather large, a clear tendency can be observed. An increase in θ -value corresponds with an increasing bed material diameter. In TABLE IV the mean θ -values and the standard deviations have been summarized for the various D_{50} 's tested.

D ₅₀	θ(mean)	standard		
(μm)	(°)	deviation (⁰)		
87	-20	17		
125	- 4	-		
185	36	7		
250	65	13		
465	83	_		

Fig. 5 gives a graph of that relationship.

TABLE IV Effect of D_{50} on θ .

It is felt to be very unlikely that a real constant 0-value exists for a specific bottom material. Thus, for instance to be irrespective of the actual order of magnitude of the water motion. During the preparation of this paper various attempts have been made to find a sounder physical basis for the observed differences; all attempts have been in vain however.

Nielsen (1979) proposes a computing method for this type of tests. In his Ch. 7 he compares his computing method with one of the Vellinga (1975) tests. (Not given in this paper since here only tests with T=1.7 s have been summarized; that particular test had a wave period of T=1.5 s). The Nielsen comparison is not that bad at a first glance (Fig. 7.6 of Nielsen's thesis). However Nielsen made a factor-5 mistake in plotting Vellinga's results. Although Nielsen's method is not entirely reliable, a comparable tendency can be distracted from his method with respect to the effect of D_{50} on θ . The authors did not work this out quantitatively for the present tests.

4.2. Transport as function of \hat{u}_1 , \hat{u}_2 and γ

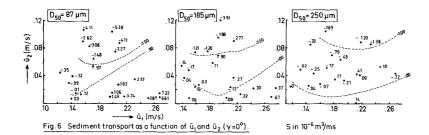
In a specific test the two transport parameters, \overline{s} and \hat{s} , and the four velocity parameters, \hat{u}_1' ; \hat{u}_1^{\star} ; \hat{u}_2' and \hat{u}_2^{\star} , can be observed. To find relationships between these is the aim of this section.

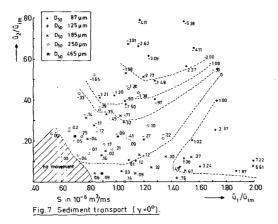
It seems attractive to start with the assumption that the mean sediment transport $\overline{\mathbf{S}}$ is directly related to the constant part of the water motion; e.g. the combination of both Stokes components $\hat{\mathbf{u}}_1'$ and $\hat{\mathbf{u}}_2'$. As an extension of this assumption the varying part of the transport, $\hat{\mathbf{S}}$, could depend (among others) on the $\hat{\mathbf{u}}_1^{\mathbf{x}}$ - and $\hat{\mathbf{u}}_2^{\mathbf{x}}$ -components. For the \mathbf{D}_{50} = 250µm bottom material, Bijker, Van Hijum and Vellinga (1976) worked out these assumptions. They found rather simple linear relationships. The results of the tests with other \mathbf{D}_{50} 's (see TABLE I), however, did not yield satisfying results. Also the approach of Bijker et al, to introduce the acceleration and deceleration of the water motion as important parameters to quantify the magnitude of $\hat{\mathbf{S}}$, did not hold for the other \mathbf{D}_{50} 's.

Therefore the foregoing approach has been abandoned in the further analyses. The four wave velocity parameters have been combined to calculate the actual velocities as a function of x. Three parameters viz.: \hat{u}_1 , \hat{u}_2 and γ result in that case. In Fig. 3 the resulting function $\gamma(x)$ belonging to the approximated \hat{u}_1 —and \hat{u}_2 —curves has been given also. At any position x, one sediment parameter S and three velocity parameters have to be taken into account now. An idea of the influence of the various velocity parameters can be obtained by taking one constant and the other two varying. Let us assume for instance $\gamma = 0^\circ$; thus at the x-positions where \hat{u}_1 (max) = $(\hat{u}_1^* + \hat{u}_1^*)$ and \hat{u}_1 (min) = $(\hat{u}_1^* - \hat{u}_1^*)$ do occur. The corresponding \hat{u}_2 —values are $(\hat{u}_2^* - \hat{u}_2^*)$ and $(\hat{u}_2^* + \hat{u}_2^*)$ respectively.

Every test then "contributes" two points to a \hat{u}_1 - \hat{u}_2 versus S graph. Fig. 6 shows the result for the various bottom materials for the choice of γ = 0°.

In particular for the \mathbf{D}_{50} = 87µm-plot of Fig. 6, a positive and a negative transport part of the $\hat{\mathbf{u}}_1$ - $\hat{\mathbf{u}}_2$ -plane can be noted and further it can be detected that some tendencies in the sediment transport do occur in the $\hat{\mathbf{u}}_1$ - $\hat{\mathbf{u}}_2$ -plane. Furthermore, it can be seen from Fig. 6 that the boundary between positive and negative transports shifts to higher $\hat{\mathbf{u}}_1$ -values as the bottom material diameter increases. This makes it attractive to see what happens when the $\hat{\mathbf{u}}_1$ - and $\hat{\mathbf{u}}_2$ -values are made





dimensionless and the various bottom materials are combined. Fig. 7 shows the result. The $\hat{\mathbf{u}}_1$ - and $\hat{\mathbf{u}}_2$ -values were divided by the critical orbital velocities for the various materials: $\hat{\mathbf{u}}_{im}$. The initiation of motion values for a flat horizontal bed were computed according to Swart's (1977) formula:

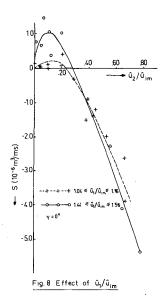
$$\hat{\mathbf{u}}_{im} = 4.58 \, \mathbf{p}_{50}^{0.38} \, \mathbf{r}^{0.043}$$
 (12)

where: $\hat{\mathbf{u}}_{im}$: initiation of movement-orbital velocity near the bed and T: wave period.

Although in Fig. 7 some measuring points fall outside the general trends and although in some parts of the \hat{u}_1/\hat{u}_{im} - \hat{u}_2/\hat{u}_{im} -plane the measuring points are rather scarce, it seems permitted to draw "iso-transport-lines".

The complex character of the net sediment transport due to waves can be seen clearly from vertical cross-sections in figures like Fig. 7. A vertical cross-section means a constant \hat{u}_1 -value and a varying \hat{u}_2 value. Let us take for example such a cross-section at 1.50 at the \hat{u}_1/\hat{u}_{im} -ordinate. Starting at $\hat{u}_2/\hat{u}_{im}=0$ (a pure sine-wave!) a sediment transport of S = 0 can be expected. A slight increase of the \hat{u}_2/\hat{u}_{im} -value yields positive transports and a further increase of the \hat{u}_2/\hat{u}_{im} -value results, after first reaching S = 0 again, in negative transports. By taking a vertical cross-section at $\hat{u}_1/\hat{u}_{im}=1.1$ in Fig. 7 for instance, an other picture results. In Fig. 8 the outcome is given for vertical cross-sections for measuring points in the ranges $1.04 \leq \hat{u}_1/\hat{u}_{im} \leq 1.16$ and $1.44 \leq \hat{u}_1/\hat{u}_{im} \leq 1.56$. For small \hat{u}_2/\hat{u}_{im} -ratios the differences are significant; for larger values of \hat{u}_2/\hat{u}_{im} it is remarkable that the differences in net transport are rather small, not withstanding the great differences in \hat{u}_1 -values.

The foregoing results hold for $\gamma = 0^{\circ}$. Similar results can be found for other γ -values. In Fig. 9 a review is given of vertical cross-sections in plots like Fig. 7 for points in the range $1.04 \leq \hat{u}_1/\hat{u}_{im} \leq 1.16$ for different values of γ . In some cases the measuring points



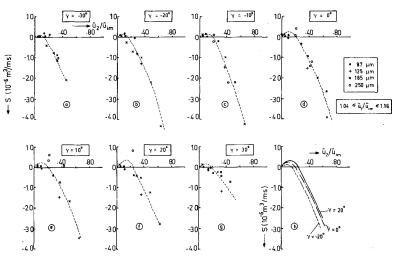


Fig.9 Effect of γ.

of the tests with different D₅₀'s coincide fairly well. Sometimes however, a systematic difference between the various D50's seems to appear. The variation of the phase shift θ as a function of D_{50} (see section 4.1) can be the reason for these discrepancies. This means in fact, that it is not allowed to consider the various D50's together as is proposed in this section by dividing the orbital velocity components by the critical orbital velocity. As a preliminary analysing method, however, the results are not that bad. The curves in Fig. 9 are roughly sketched curves. In Fig. 9h an idea of the effect of the γ -value can be observed. The effect seems to be rather small. The unsolved dependence of the sediment transport as functions of the parameters \hat{u}_1 , \hat{u}_2 and γ (see Figs. 8 and 9) makes it unrealistic to believe in the reliability of the simple cosine function as an approximation of the sediment transport as a function of x (Eq. 10). An iterative method can be used to arrive at a more reliable and a more complicated transport function. Due to insufficient data this has not been carried out in the present paper.

5. Discussion

The outcome of the series of small-scale tests with different D50's has brought some surprising facts. As could be seen in section 4 the preliminary analyses did not solve the problems. Some results have been "seen" without, till now, understanding "why". This is rather disappointing since in the tests, in fact a very simple mode of onshore-offshore sediment transport (regular waves; horizontal bed) was considered. Even these simple tests yielded rather complicated results with clear tendencies as indicated for instance by the Figs. 5, 7 and 9. The authors tried to explain some tendencies qualitatively by taking into account the description of the actual transport by vortex formation and vortex ejection etc. as presented by Bijker et al (1976) and Nielsen (1979). They did not succeed. To find some more data just by carrying out more test with other velocity combinations is rather simple. Extended, and probably more reliable, graphs will result. However for direct practical use those graphs are useless. The velocity ranges as well as the set-up of these tests, e.g. a horizontal bed,

are quite different in prototype conditions. For a further increase in insight in the onshore-offshore transport mode a quantitative idea of concentration and velocity field as a function of time will be necessary. At the Delft University we intend to go that long road.

6. Summary and conclusions

- Small-scale tests with progressive waves over a horizontal bed in a flume with different D₅₀'s as bottom material show a net sediment transport which depends apparently on the water motion.
- The water motion, approximated by the first and the second harmonic component of the horizontal orbital velocity component, and the phase angle between both components, has been related to the sediment transport. Rather complex, till now not comprehended, predictive curves can be distracted from the measurements.
- These predictive curves show clear tendencies. The predictive curves, however, can hardly be used for practical purposes.
- The bed material diameter is an important parameter in the sediment transport process. A remarkable shift occurs in the position of the top of the S-curve with respect to the top of the orbital component curves when different D_{50} 's are used.
- To some degree the effect of the diameter of the bottom material can be taken into account by dividing the orbital velocity components by the critical orbital velocity (= maximum orbital velocity at the bed at initiation of movement).

References

Vellinga, P. (1975)

Bijker, E.W.; Hijum, E. van; Vellinga, P. (1976) Sand transport by waves Proc. 15th Coastal Eng. Conf., Honolulu Vol II, Chap. 68 Buhr Hansen, J. and Svendsen, I.A. (1974) Laboratory generation of waves of constant form Proc. 14th Coastal Eng. Conf., Copenhagen Vol I, Chap. 17 Fontanet, P. (1961) Théorie de la génération de la houle cylindrique par un batteur plan La Houille Blanche, nr 1 et 2. Hulsbergen, C.H. (1974) Origin, effect and suppression of secondary waves Proc. 14th Coastal Eng. Conf., Copenhagen Vol I, Chap. 22 Kravtchenko, J.; Santon, L. (1957) Nouvelles recherches sur la houle de laboratoire 7th General Meeting, I.A.H.R. Vol. II Nielsen, P. (1979) Some basic concepts of wave sediment transport Thesis, Institute of Hydrodynamics and Hydraulic Engineering Technical University of Denmark, Lynghy Schepers, J.D. (1978) Zandtransport onder invloed van golven en een eenparige stroom bij variërende korreldiameter Craduation thesis, Delft Univ. of Tech. (in dutch) Skjelbreia, L. (1958) Gravity waves; Stokes third order approximation, tables of functions Berkeley, Calif .: The Engineering Foundation Council on Wave Research Swart, D.H. (1974) Offshore sediment transport and equilibrium beach profiles Delft Hydraulics Laboratory, Publ. No 131, Delft Swart, D.H. (1976) Predictive equations regarding coastal transports Proc. 15th Coastal Eng. Conf., Honolulu Vol II, Chap. 66 Swart, D.H. (1977) Weighted value of depth of initiation of movement Stellenbosch, Aug. Tilmans, W.M.K. (1979) Zandtransport in de golfrichting in relatief ondiep water Craduation thesis, Delft Univ. of Tech. (in dutch)

Zandtransport door golven en de invloed van stoorgolven Craduation thesis, Delft Univ. of Tech. (in dutch)